PHYSICAL REVIEW B, VOLUME 64, 041201

Combined optical and microwave approach for performing quantum spin operations on the nitrogen-vacancy center in diamond

Forrest T. Charnock and T. A. Kennedy
Naval Research Laboratory, Washington, D.C. 20375
(Received 9 March 2001; published 29 June 2001)

Electron spin echoes were performed on nitrogen-vacancy (N-*V*) centers in diamond using optical polarization and detection and 35 GHz microwave control. The experiments demonstrate an approach to quantum information in the solid state. A phase memory time of 3.6 μs was measured, and coupling of the electronic spin to the ^{14}N nuclear spin was observed. Because of the favorable properties of the N-*V* center, interesting extensions of these single-qubit operations can be proposed.

DOI: 10.1103/PhysRevB.64.041201 PACS number(s): 76.30.−v, 03.67.−a, 81.05.Uw

Following the suggestion of quantum information and the discovery of efficient quantum algorithms, demonstrations of quantum operations and computing have been performed using atoms in cold traps and NMR of simple molecules.[1] While these have been striking and instructive, there are many incentives to develop quantum gates in the solid state. The requirement of discreet energy levels leads to imperfect or structured materials; hence, the spin states found in defects and quantum dots have been proposed to explore quantum information based on solid-state devices.

The nitrogen-vacancy (N-*V*) center found in irradiated type-Ib diamond is a prominent candidate. It consists of a nitrogen substituting for a carbon plus a nearest-neighbor vacancy. [See Fig. 1(a).] These centers are created with high-energy electron radiation followed by thermal annealing.[2,3] They have a ^3A ground state (electronic spin of 1) and a ^3E excited state. The optical transition between these states has a very high quantum efficiency,[2] which has allowed single-defect spectroscopy to be performed both at low and room temperatures.[4,5] Previous work at zero and small magnetic fields has found the ground state to have a spin coherence lifetime of 4.5–80 μs.[6–10] These robust optical and spin properties have led to suggestions for utilizing the N-*V* center as a quantum gate with optical addressing and control.[11,12] Recently, the spin coherence has been further probed with coherent Raman spectroscopy with an eye toward single qubit preparation and operations.[13]

In this work, we explore quantum operations on ensembles of N-*V* centers using a combined optical/microwave approach. The state is prepared and read out optically, thus maintaining the sensitivity required for single-qubit operations. Coherent control is achieved with microwave pulses. The experiments, performed at fields near 1 T, measure the phase memory time and reveal modulation of the electron coherence by the ^{14}N nuclear spin. The experiments provide a model for quantum information processing in the solid state. The N-*V* center itself displays properties that set a standard for a solid-state qubit.

Our experimental conditions were as follows. All measurements were performed at pumped liquid-He temperature ($\sim$1.4 K). An Oxford Instruments split coil superconducting magnet supplied the external field for the magnetic resonance. The sample is a Sumitomo diamond ($1.7\times3.5\times3.5$ mm^3) that was electron irradiated and annealed; the total nitrogen concentration is 200 ppm ($\pm$20 ppm), and the concentration of N-*V* centers is 20 ppm ($\pm$7 ppm). It was held in a resonant microwave cavity with optical access, and the magnetic field was oriented parallel to the $\langle 110\rangle$ crystal direction. A fast PIN diode switched the output of the 35-GHz microwaves generated by a free running GUNN oscillator or an HP83650A microwave synthesizer. The PIN was controlled via an Interface Technology RS690 250-MHz digital word generator. To amplify the short pulses needed for the coherent operations, we added a 10-W Hughes 8000H TWT amplifier. Optical excitation came from a cw Millennia

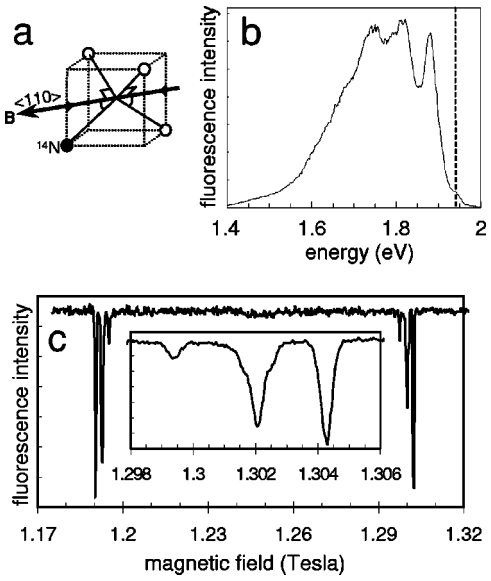

FIG. 1. Photoluminescence and ODMR from the N-*V* center in diamond. (a) illustrates an N-*V* center with its axis 35° to the applied field; the empty circles are carbons. In the photoluminescence spectrum of the sample (b), the dotted line marks the position of the zero phonon line at 1.945 eV. In the ODMR (c), there are two sets of lines at 1.2 and 1.3 T; the inset shows a detail of the upper set of lines. Each line is about 0.5 mT wide. The applied magnetic field was tilted from the $\langle 110\rangle$ crystal axis by one or two degrees; this shifted the resonance positions enough to easily distinguish the lines for those centers oriented near $\pm$35° from **B**.

Xs solid-state laser running at 532 nm. The fluorescence from the sample was focused onto a Si photodiode, and the output was measured with a lock-in amplifier.

Conventional photoluminescence and optically detected magnetic resonance (ODMR) provide the optical and magnetic parameters necessary for the coherent experiments. The photoluminescence spectrum is broad due to vibronic coupling of the lattice with the zero phonon line (ZPL) at 1.945 eV. [See Fig. 1(b).] The ZPL arises from transitions between the ^3E excited state and ^3A ground state.[2,4,7] This transition is spin selective and creates a spin-polarized population in the ground state after a characteristic time T_1'. T_1' is determined by the light intensity, optical selection rules, and lifetimes; in our case, it is about 1.3 ms. Once this spin polarization is present, spin transitions can be observed with ODMR. When illuminated with resonant microwaves, the fluorescence intensity will change as the spin population moves to or from optically active spin levels. We performed ODMR by switching the microwaves on and off at 500 Hz and monitoring the fluorescence intensity parallel to the magnetic field. With the applied field near the $\langle 110 \rangle$ crystal direction, resonance is observed as a drop in the fluorescence. [See Fig. 1(c).] This revealed two sets of lines corresponding to transitions between adjacent electronic spin states. Most of the observations are described by the Hamiltonian

$$\mathcal{H}_e = (g\beta)\mathbf{B}\cdot\mathbf{S} + D\left[S_z^2 - \frac{1}{3}S^2\right],$$

with D (the splitting due to the axial crystal field) and g in agreement with previous work.[14] Each set consists of three lines arising from the four possible orientations of the principal defect axis ($\langle 111 \rangle$ directions) with respect to the applied magnetic field. [See Fig. 1(a).] Rotation studies showed that the outer lines arise from those defects oriented approximately $\pm 35°$ from the applied field, and the inner line arises from the pair of centers oriented approximately 90° from the field. The shoulders on the 90° line indicate that some centers sense crystal fields with lower than axial symmetry.[4]

If we replace the slow microwave modulation with fast intense pulses, we can detect electron spin echoes. These are formally equivalent to single qubit operations and were realized as follows. First, we set the magnetic field on the nondegenerate resonance shown at 1.299 T. After a period T_1', cw laser illumination created a spin-polarized population in the $m_S = 0$ state. Next, we operated on the polarization by applying to the sample a sequence of three, short, intense, microwave pulses. [See inset of Fig. 2(a).] The first, a $\pi/2$ pulse, rotated the magnetization into a coherent superposition of the $m_S = 0$ and -1 states. After a period t_0, a π pulse inverted the spins and they refocused at a time $2t_0$. A final $\pi/2$ pulse rotated the spins back to the original spin state. If the spin echo were perfectly generated, the final spin polarization would match the initial spin polarization, and the observed fluorescence would have remained constant. However, as mistimed pulses or spin decoherence processes prevented some of the spins from returning to the original state, the spin polarization decreased after the pulse sequence. This caused the fluorescence intensity to decrease.

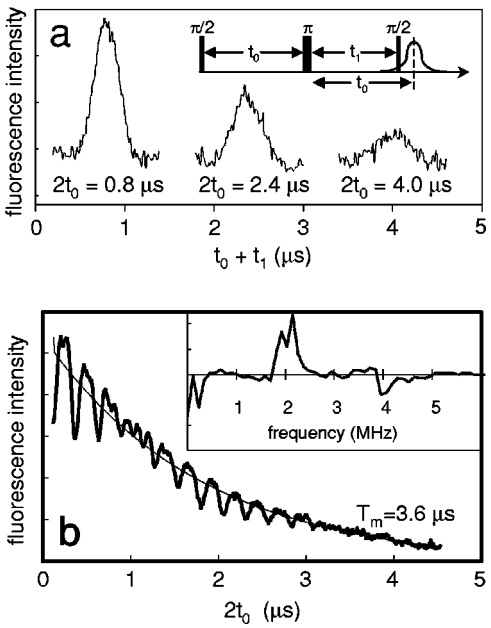

FIG. 2. Optically detected spin echoes and the envelope of the spin echo decay. In (a), the inset illustrates the pulse sequence used. (b) shows the spin echo decay envelope with nuclear modulation; the overall decay of the envelope is 3.6 μs. The inset shows the cosine Fourier transform of the modulation.

The experimental results are described as follows. Sixteen watts of peak power into the microwave cavity generated π pulses of 48 ns. The pulse sequence was repeated at 500 Hz. We detected the fluorescence with a Si photodiode and a lock-in (identical to the ODMR detection). The outline of the spin echo was observed by sweeping the position of the final pulse across the refocusing point at $2t_0$. [See Fig. 2(a).] With different initial delays, the echo moved to longer times and decreased in amplitude.

We observed the envelope of the spin echo decay by holding the delays between the pulses equal ($t_1 = t_0$) while sweeping both delay times. [See Fig. 2(b).] When the resonance at 1.299 T was selected, this revealed a modulated decay curve with a phase memory time (T_m) of 3.6 μs. Similar results were found when the resonance at 1.195 T was observed. Since an exponential function well describes the overall decay, T_m is equivalent to T_2 as defined by the Bloch equations.[15] Electron spin echo envelope modulation (ESEEM) is frequently observed in coherent studies; it usually arises from interaction between the electronic spin and a nuclear spin.

The measured phase memory time can be attributed to dipole-dipole interactions with other N-V centers. The density of N-V centers in our sample is roughly 20 ppm; however, the density of centers with a given orientation is only one quarter of this: 5 ppm. This yields a mean separation between equivalent centers of 10 nm. The intensity of the magnetic dipole field induced by one center on a neighbor (ignoring the angular dependence) is

$$B \approx \frac{g\beta}{r^3},$$

in our case about 1.6 μT. This creates an homogeneous linewidth of 50 kHz or a spin lifetime of 20 μs. This is remarkably close to our measured value of T_m.

Other measurements on other samples have revealed somewhat longer times. Measurements based on Raman-heterodyne spectroscopy (RHS) with **B** near the $(m_S=-1)/(m_S=0)$ crossover at 102.8 mT give dephasing times from 4.5 to 8.0 μs.[7–9] Longer times, from 41 to 80 μs, were reported from coherent ODMR at small but finite fields.[6,10] Although the concentrations of N-*V* centers for samples used in these other works were not given, it is likely that they were lower than in our sample and that spin-spin interactions determine the lifetime in each case.

Once the overall echo decay is subtracted, the modulation can be analyzed to reveal its harmonic content. A cosine Fourier transform of the modulation reveals two primary frequencies of 1.9 and 2.2-MHz. [See inset of Fig. 2(b).] The source of the modulation is usually a nuclear spin[16] and, because of the structure of the defect, the ^{14}N$(I=1)$ is the prime candidate.

To observe ESEEM, two conditions must be fulfilled.[17] First, the hyperfine levels of one electronic spin state must be coupled with more than one hyperfine state of the other electronic level. For ^{14}N, this mixing of the nuclear states requires that the nuclear Zeeman energy be comparable to the anisotropic hyperfine interaction or the quadrupole interaction. The second condition is that the nutation rate of the electronic spin is large compared to the nuclear resonance frequencies. With a 48-ns π pulse, the nutation rate is 10 MHz.

The nuclear spin Hamiltonian describing the ground state of this center is[7]

$$\mathcal{H}_n = A_\parallel S_z I_z + \frac{1}{2}A_\perp (S^- I^+ + S^+ I^-) - (g_n\beta_n)\mathbf{B}\cdot\mathbf{I} + P\left[I_z^2 - \frac{1}{3}I^2\right].$$

Here, β_n is the nuclear magneton; $A_\parallel$ and $A_\perp$ are the hyperfine constants perpendicular and parallel to the defect axis ($\langle 111\rangle$); and P is the quadrupole splitting. For ^{14}N, $g_n\beta_n = 3.07$ MHz/T. The hyperfine interaction has been observed with electron paramagnetic resonance (EPR) providing a measurement of $A_\parallel = 2.3$ MHz.[14] The RHS measurements[7] confirm $A_\parallel$ and give $A_\perp = 2.1$ MHz and $P = -5.04 \pm 0.05$ MHz. In our case with applied fields around 1 T, the hyperfine and quadrupole interactions are comparable to the nuclear Zeeman interaction and strong mixing occurs. Thus it is likely that the observed modulation is due to ^{14}N ESEEM.

In order to verify these assignments, we have calculated the ESEEM frequencies using a diagonalization of the full electronic and nuclear Hamiltonian. The 9×9 matrix manipulations were done with MATHCAD. Using the parameters from the EPR and RHS work, we get frequencies that are higher than the measured frequencies. As a check of our calculations, we verified that the parameters do give the frequencies measured in the RHS work.

It is likely that the ESEEM and RHS techniques sample different parts of the distribution of strained N-*V* centers. Dräbenstedt *et al.*[5] observed that the different spectroscopic techniques sense N-*V* centers under particular strain conditions. For a sample with a relatively high concentration of defects (10^{16} cm^{-3} or more), there is considerable inhomogeneous broadening of the resonance lines; those defects under the greatest strain lie in the wings of these lines. He *et al.*[7] reported that their Raman-heterodyne signal was centered on the low-energy side of the inhomogeneously broadened optical line; hence, their Hamiltonian parameters describe centers with a particular strain. Since we have used nonselective excitation, the sharper unstrained defects dominate our observations.

With its high quantum efficiency and long spin lifetimes, the N-*V* center serves as a model qubit and shows potential for future quantum information applications. Its spin coherence lifetime is much longer than those of many other semiconductor systems. By exploiting this long lifetime, we have demonstrated single qubit operations using a combined optical and microwave approach. This work can be extended to higher temperature, a two-qubit gate utilizing the ^{14}N nuclear spin, and coherent studies of single N-V centers.

A two-qubit gate would make use of both the electronic and nuclear spins in this center. At 1 T, the nuclear states remain strongly coupled by the hyperfine and quadrupole interactions. If the field were increased, the nuclear states would become purer allowing controlled entanglement following the scheme used in NMR.[18] A source of rf pulses would address the ^{14}N nuclei. This would demonstrate a controlled-NOT gate using an ensemble of N-*V* centers.

This work could also be extended to single N-*V* centers. Dräbenstedt *et al.*[5] have used confocal microscopy to observe the fluorescence of individual centers at temperatures as low as 5 K; and Gruber *et al.*[4] have performed optically detected magnetic resonance on a single N-*V* center at room temperature. Also, Wrachtrup *et al.*[19] have performed optically detected spin coherence measurements on single pentacene molecules; extending this to a single N-*V* center is certainly possible.

In summary, a combined optical and microwave approach to quantum information with the N-*V* center has been demonstrated. A long phase memory time is observed, and coupling to the ^{14}N nucleus is strong for fields near 1 T.

We thank Steve Rand of the University of Michigan for providing the diamond used in this study, and B. Danly and C. Hochuli for the pulsed microwave equipment.

[1] For a review, see C.H. Bennett and D.P. DiVincenzo, Nature (London) **404**, 247 (2000).
[2] G. Davies and M.F. Hamer, Proc. R. Soc. London, Ser. A **348**, 285 (1976).
[3] J.H.N. Loubser and J.A. van Wyk, Rep. Prog. Phys. **41**, 1201 (1978).
[4] A. Gruber, A. Dräbenstedt, C. Tietz, L. Fleury, J. Wrachtrup, and C. von Borczyskowski, Science **276**, 2012 (1997).
[5] A. Dräbenstedt, L. Fleury, C. Tietz, F. Jelezko, S. Kilin, A. Nizovtzev, and J. Wrachtrup, Phys. Rev. B **60**, 11 503 (1999).
[6] E. van Oort, N.B. Manson, and M. Glasbeek, J. Phys. C **21**, 4385 (1988).
[7] Xing-Fei He, N.B. Manson, and P.T.H. Fisk, Phys. Rev. B **47**, 8809 (1993); **47**, 8816 (1993).
[8] Keith Holliday, Xing-Fei He, Peter T. H. Fisk, and Neil B. Manson, Opt. Lett. **15**, 983 (1990).
[9] C. Wei and N.B. Manson, J. Opt. B: Quantum Semiclassical Opt. **1**, 464 (1999).
[10] M. Glasbeek and E. van Oort, Radiat. Eff. Defects Solids **119-121**, 301 (1991).
[11] M.D. Lukin and P.R. Hemmer, Phys. Rev. Lett. **84**, 2818 (2000).
[12] M.S. Shahriar, P.R. Hemmer, S. Lloyd, J.A. Bowers, and A.E. Craig, quant-ph/0007074 (unpublished).
[13] P.R. Hemmer, A.V. Turukhin, M.S. Shahriar, and J.A. Musser, quant-ph/0007114 (unpublished).
[14] J.H.N. Loubser and J.A. van Wyk, Diamond Res. **11**, 11 (1977).
[15] J.R. Norris, M.C. Thurnauer, and M.K. Bowman, Adv. Biol. Med. Phys. **17**, 365 (1980).
[16] W.B. Mims, Phys. Rev. B **5**, 2409 (1972).
[17] J. Schmidt and D.J. Singel, Annu. Rev. Phys. Chem. **38**, 141 (1987).
[18] N.A. Gershenfeld and I.L. Chuang, Science **275**, 350 (1997).
[19] J. Wrachtrup, C. von Borczyskowski, J. Bernard, M. Orrit, and R. Brown, Phys. Rev. Lett. **71**, 3565 (1993).